



Original Article

# Modelling the Dispersion of Dredged Material in Marine Environment Using Hydrodynamic and Sediment Transport Simulations in Tho Quang Port, Vietnam

Nguyen Duc Toan<sup>1</sup>, Tran Anh Quan<sup>2,\*</sup>, Trinh Thi Thuy<sup>3</sup>, Lai Duc Ngan<sup>1</sup>

*Viet Nam Agency of Seas and Islands, 83 Nguyen Chi Thanh, Lang Thuong, Dong Da, Hanoi, Vietnam*

*Hanoi University of Mining and Geology, 18 Vien, Duc Thang, Bac Tu Liem, Hanoi, Vietnam*

*Hanoi University of Natural Resources and Environment, 41A Phu Dien, Bac Tu Liem, Hanoi, Vietnam*

Received 17<sup>th</sup> December 2024

Revised 27<sup>th</sup> March 2025; Accepted 9<sup>th</sup> May 2025

**Abstract:** Maintaining navigable port channels through dredging is crucial for maritime trade, yet offshore disposal of dredged material can impact the local marine environments. This study modeled the dispersion and deposition patterns of total suspended solids (TSS) resulting from the disposal of dredged sediments at an offshore site near Tho Quang Port, central Vietnam. An advanced coupled numerical modeling system integrating hydrodynamics, spectral waves, and sediment transport processes was developed using the MIKE modeling suite. Extensive field data was collected and used for model parameterization, boundary conditions, and rigorous validations, including bathymetry surveys, acoustic doppler current profiler measurements, tide gauge data, and sediment sampling/characterization like grain sizes, densities, settling velocities. Simulations over a 45-day construction period represented extreme scenarios under contrasting Southwest and Northeast monsoon conditions. The model results showed that the highest TSS concentrations, above 0.05 kg/m<sup>3</sup>, were restricted to an area within 12 km of the disposal location. However, the 0.015-0.02 kg/m<sup>3</sup> contour extended further along the predominant northwest-southeast dispersion axis aligned with prevailing winds and currents, reaching 12-18 km. Seabed accumulation patterns showed a radially symmetrical cone with maximum thicknesses of 0.5 m proximal to the release site. The 0.1 m deposition footprint spanned 102-122 ha due to asymmetric sediment advection by the contrasting monsoon forcings. Key factors governing the dispersion and accumulation patterns included sediment characteristics, hydrodynamics (tides, currents, waves), wind forcing, and bathymetry. TSS plumes and sedimentation footprints were constrained, suggesting disposal impacts may be localized around the authorized site during operations based on the limited dispersion predicted.

\* Corresponding author.

E-mail address: [quantrananh.humg@gmail.com](mailto:quantrananh.humg@gmail.com)

<https://doi.org/10.25073/2588-1094/vnuces.4410>

This study highlights the value of integrated numerical modeling for quantitatively forecasting the environmental impacts of dredged material disposal. Such predictive insights can guide monitoring programs, ecological risk assessments, and the development of mitigation strategies to balance infrastructure growth with environmental protection goals for coastal regions.

*Keywords:* Submersion; environmental modeling; sediment dredging; TSS dispersion; seabed occupation.

## 1. Introduction

In recent decades, seabed dredging has become a vital activity for the management and functioning of ports across Vietnam [1-3]. Removing sediment, sand, and debris from the seafloor is crucial for maintaining or deepening navigation channels, enabling the safe passage of vessels and the steady flow of cargo [4]. The port of Tho Quang in central Vietnam serves as a key regional hub, and its dredging efforts are integral to smooth operations. In 2022, the Tho Quang shipping channel dredging project was initiated to enhance navigational safety within the port by dredging 180,000 m<sup>3</sup> of sediment to a depth of -10 m along the approach channel and turning basin. To mitigate environmental impact, dredged material was relocated 45 km away per approval from the Da Nang Provincial People's Committee. The designated dumping site spanned 150 ha, sanctioned by the local government (Figure 1). Proper execution of this project supported the ongoing success and growth of Tho Quang port.

Rising maritime traffic has necessitated dredging at Tho Quang. With expanding global trade, more ships enter and leave ports worldwide. To accommodate this demand, dredging deepens channels to allow larger vessels [5, 6]. Another factor is sedimentation, which can obstruct navigation [7, 8]. Accumulated sediment reduces channel depth, while shoal formation endangers port operations. Regular dredging removes this sediment to maintain depth and navigability [2, 9, 10]. Further, dredging enables channel maintenance by clearing sediments and hazards for safe, efficient shipping [11, 12]. As Vietnam confronts intensifying climate change impacts like sea level rise and extreme weather events

[13-15], comprehensive research on sustainable dredged material disposal practices is becoming increasingly crucial [16]. Potential sea level rise associated with continued global warming poses significant threats to coastal regions, potentially exacerbating sedimentation rates and necessitating more frequent dredging to maintain navigational channels [4, 6, 17, 18].

The disposal of dredged material in marine environments is a common practice worldwide, including at ports in Vietnam, which involves the deposition of sediment, sand, and debris removed during dredging operations. While this practice serves essential purposes such as maintaining safe and efficient navigation, protecting marine habitats, and managing dredging waste [19, 20], there are growing concerns regarding the ecological impacts associated with the disposal of dredged material. One of the primary issues is the dispersion of total suspended solids (TSS), which can have detrimental effects on aquatic life and human well-being [19, 21, 22]. Despite the importance of this issue, research on TSS dispersion remains limited, emphasizing the need for further investigation.

Recent studies have made significant contributions to understanding TSS dispersion dynamics following dredged material disposal. Cox et al., [18] investigated TSS dispersion after dredged material dumping offshore of Tuban in East Java, observing a sharp increase in TSS concentrations around the dumping site, with elevated levels persisting over time. Their findings highlighted the influence of currents on the dispersion of TSS, providing valuable insights into these processes. Similarly, Quan et al., [23] examined TSS dispersion from dredged material dumping off Vung Tau Port, noting a

spike in TSS concentrations immediately following dumping, with the highest concentrations observed near the disposal site. As the material dispersed, TSS levels gradually decreased, offering insights into the temporal aspects of TSS dispersion.

While these studies have advanced our understanding of TSS dispersion in the water column, there is a critical lack of research investigating the resulting sedimentation dynamics on benthic environments. The scientific literature examining sediment accumulation patterns, spatial footprints, and physicochemical transformations on the seafloor in response to dumped dredged materials is extremely limited [4, 23-25]. This knowledge gap represents a significant barrier to developing science-based policies and best practices for sustainable dredging and disposal operations, given the vulnerability of seafloor habitats and communities to anthropogenic disturbances [21, 22, 26].

To address this research need, dedicated studies are urgently required to characterize the physical dispersion of dredged material in marine environments. Key aspects that demand investigation include quantifying sediment transport rates, mapping the spatial extent and concentration gradients of suspended materials, analyzing particle size distributions and geochemical properties of dispersed sediments, and assessing the temporal evolution of these plumes [9, 23, 27]. A comprehensive understanding of these dispersion dynamics is essential for informing monitoring programs, predicting sediment fate, and formulating effective dredging and disposal strategies [28, 29]. This research explores TSS dispersion and sedimentation resulting from the immersion of dredged material in Tho Quang port. Employing the MIKE modeling system and observational data, the study simulated the TSS immersion process, providing essential perspectives on the scope and intensity of sediment propagation at the dredging and immersion sites. By investigating the physical processes associated with dredged material disposal and the

substantial effects of such disposal on hydrodynamics and sediment transport, the research supplies valuable insights for pertinent regulatory bodies. These insights can empower these agencies to make well-informed decisions regarding port dredging practices and the implementation of effective sediment management measures.

## 2. Study Area and Methods

### 2.1 Study area

The study focuses on the navigation channel to Tho Quang Port in Da Nang, Vietnam. Da Nang is a coastal city in central Vietnam, experiences a tropical monsoon climate with distinct wet and dry seasons. Its weather is shaped by its location between the Annamite Mountains and the East Sea. Two monsoons shape the region's seasons: the Northeast monsoon (October to March) brings cool, dry air, while the Southwest monsoon (May to September) brings warm, humid air. These monsoons create a dry season with temperatures of 19-24 °C and minimal rainfall, and a wet season with temperatures of 25-35 °C and heavy precipitation, respectively. Annual rainfall averages 2,000 mm, peaking in September and October. Da Nang's tides are primarily diurnal, with a moderate range of 0.5-1.5 m. Wave patterns align with the monsoons: northeasterly waves of 1-2 m during the dry season, and easterly to southeasterly waves in the wet season. Typhoons, most common from September to November, can generate waves exceeding 4-5 m, posing risks to coastal areas.

The Tho Quang port navigation channel is designed for one-way maritime traffic accommodating vessels up to 10,000 DWT. Despite historical use within natural depth parameters, varying from 2.7 to 4.5 m, certain segments near the Son Tra integrated port area present shallower depths. The channel, allowing vessels with a draft of 3.5 to 4.0 m, is undergoing a significant renovation and upgrade, covering approximately 2,927 m. This includes two key

sections (Figure 1) catering to different vessel capacities, and the dredged material generated, totaling 654,510 m<sup>3</sup>, will be responsibly disposed of at sea. The designated dumping location, spanning 150 ha, has received official

approval from the People's Committee of Da Nang city, signifying a critical area undergoing transformation to meet evolving navigational and environmental needs.

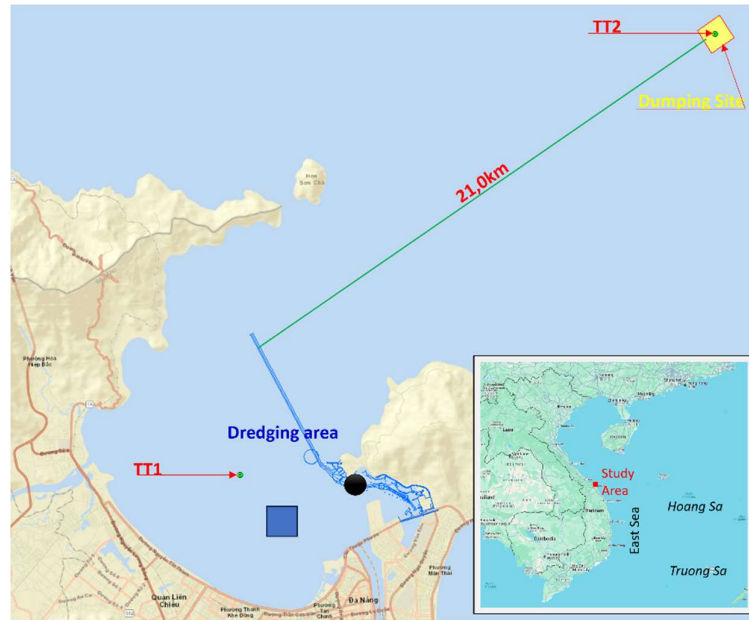


Figure 1. Map of the study area. The small rectangle indicates the designated submersion site for dredged material from Tho Quang Port. Wave measurement locations, TT1 and TT2, are marked with green dots and sediment sample locations with blue squares.

## 2.2. Integrated Hydrodynamic and Sediment Transport Modeling

To accurately simulate the intricate processes of sediment transport, erosion, and deposition of non-cohesive sediment in both marine and freshwater environments, we utilized the cutting-edge simulation tool, MIKE 21MT [30]. Widely adopted for modeling hydrodynamic and water quality processes in aquatic settings, the MIKE model assumes steady-state or quasi-steady-state flow conditions, uniform sediment properties, and a consistent bed when investigating sediment dispersion. Figure 2 illustrates the working flow of the simulation. The transport TSS released from dredging operations was simulated using a suite of hydrodynamic and sediment transport

models. The MIKE 21 spectral wave (SW) model was first applied to generate wave parameters, while the MIKE 3 hydrodynamic (HD) model was used to compute currents and water levels. The SW and HD models provided the necessary hydrodynamic inputs to drive the MIKE 3 mass transport (MT) model, which represented the processes of advection, dispersion, and settling that govern TSS transport. Concentrations of TSS from the dredging activities were simulated by introducing a TSS load into the MT model at the defined dumping location and schedule. The coupled MIKE 21 SW, MIKE 3 HD, and MIKE 3 MT modeling suite enabled dynamic simulation of the dispersion of the turbid dredged material plume based on complex hydrodynamic conditions in the study area.

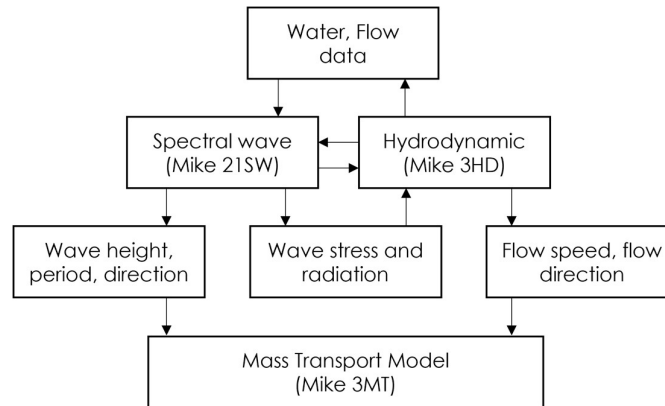


Figure 2. Schematic view of simulation process.

### 3. Data Collection and Model Setup

#### 3.1. Topographic, Meteorological, Hydrological and Oceanographic Data

Bathymetric data utilized in this study were obtained from multiple sources to provide comprehensive geographical coverage of the modeling domain. Regional seabed topography was represented using the General Bathymetric Chart of the Oceans (GEBCO) global dataset, which show ocean bathymetry at a 15 arc-second resolution (Figure 4a). For nearshore areas, higher-resolution topographic maps at 1:50,000 (Figure 3) and 1:25,000 scales were acquired from the Ministry of Natural Resources and Environment and integrated to better capture the complex bathymetry of the coastal zone (Figure 4b). Additionally, recent in situ bathymetric measurements conducted in 2021 supplied detailed topographic insights surrounding the proposed dredged material disposal site. The combination of open-access databases and field surveys provided a strong and accurate representation of the seabed at both regional and local levels, which is important for modeling water movement and sediment spread.

We used the WAVEWATCH III dataset developed by NOAA to improve our understanding of wave dynamics in the study area. This high-resolution, globally recognized dataset complements local measurements by

providing broader spatial coverage and long-term records of wave parameters, including significant wave height, peak period, and directional spectra for the model's north, east, and south boundaries (Figure 4a). Integrating WAVEWATCH III data with field surveys ensured a comprehensive and accurate representation of environmental conditions for modeling hydrodynamics and sediment dispersion in the coastal zone. For wind data, we used the ERA5 dataset provided by the European Centre for Medium-Range Weather Forecasts (ECMWF). ERA5 offers global, hourly estimates of wind parameters with a spatial resolution of 0.25°.

High-resolution hydrodynamic data were acquired to characterize local currents, waves, and water levels. Hourly water levels were measured using tide gauges deployed at two coastal locations (Figure 1) during April 15–24, 2023 (at TT1), and January 16–24, 2024 (at TT2). The collected data included significant wave height, period, and direction; current velocity and direction at three layers (surface, middle, and bottom); and water levels. These datasets were used for model calibration to ensure an accurate representation of hydrodynamic conditions. Acoustic Wave and Current profilers were utilized to measure vertical profiles of currents throughout the water column, yielding comprehensive empirical data on current velocities across the modeling domain

over the survey period. The combined hydrodynamic measurements supplied key inputs to drive and validate numerical models

while offering insights into local wave, current and tidal processes operative over the dredging project timeframe.

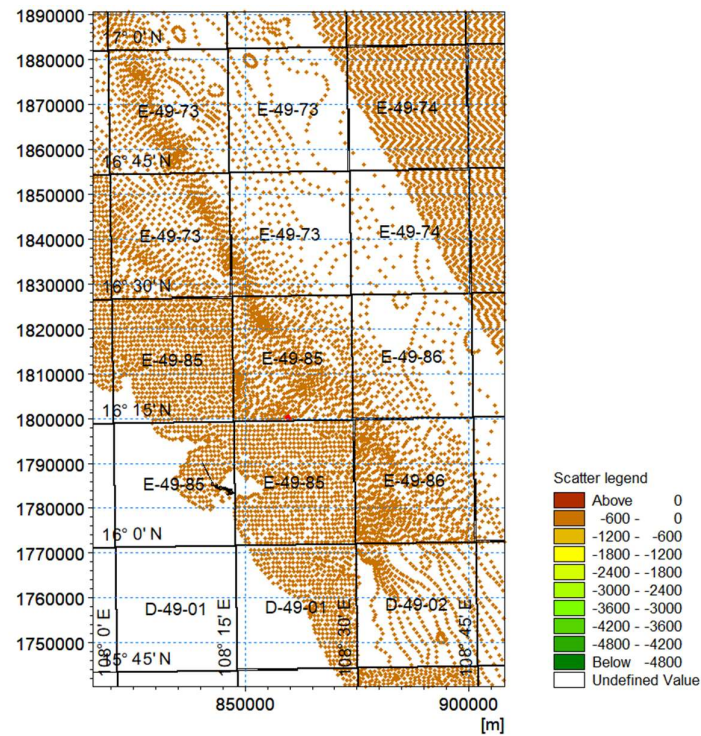


Figure 3. Fragmentation map of the seabed topography at a 1:50,000 scale used in this study.

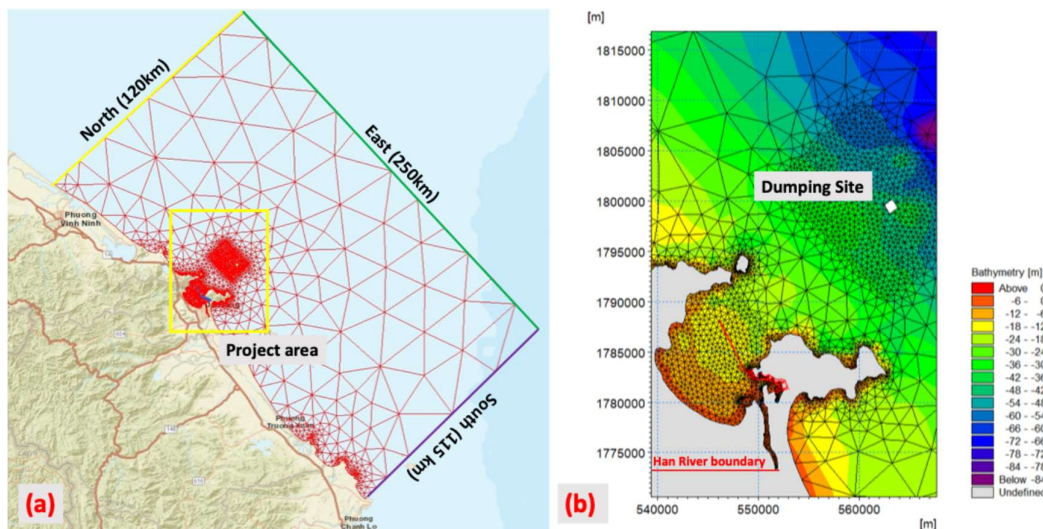


Figure 4. Computation domain with finite element grids for (a) the whole domain and (b) the port site.

### 3.2. Sediment Sampling

The sediment composition and physical properties used in the dispersal modeling were obtained from field measurements and laboratory analysis of samples ( $n=18$ ) collected across the Tho Quang Port dredging site in May 2022. These samples were analyzed to characterize sediment composition and physical attributes, such as density, settling velocity, and shear stress limits. The values for mud (density of  $1,050 \text{ kg/m}^3$ , settling velocity of  $0.015 \text{ m/s}$ , and shear stress limit of  $0.02 \text{ N/m}^2$ ) and coarse sand (density of  $2,650 \text{ kg/m}^3$ , settling velocity of  $0.3 \text{ m/s}$ , and shear stress limit of  $0.5 \text{ N/m}^2$ ) were derived directly from these analyses and are integral to modeling sediment dispersal during the dredging process. Sediment composition analysis showed that the dredged material was mainly made up of fine sand (31%), coarse sand (29%), and mud (29%), based on the median particle size distribution. This study focuses exclusively on the non-cohesive sand fraction, which plays a critical role in understanding sediment transport dynamics and potential environmental impacts of dredging operations.

### 3.3. Model Setup

#### 3.3.1. Computational Domain

The computational domain, ranging from Quang Tri Province to Binh Chau District in Quang Ngai Province, spanning 219 km, has been modeled using a finite element grid (Figure 4). The central area of focus lies around Tien Sa Port and the maritime channel of Da Nang, with extensions to both the northern and southern regions of the project area to ensure comprehensive coverage for substance dispersion. The finite element grid comprises 5,824 nodes, designed with variable resolutions tailored to specific areas of interest. Grid cell sizes range from a minimum of 40 m to a maximum of approximately 300 m, with finer resolutions applied near the dumping and dredging locations and coarser resolutions in deeper sea regions. The numerical model

employs five vertical layers for calculation purposes.

#### 3.3.2. Boundary Conditions

Boundary conditions for the Mike 3HD hydrodynamic model were defined by incorporating water level time series from the regional Mike 21 Tidal model along northern, southern, and eastern open boundaries. Besides, the wave boundary for the Mike 21SW model at the eastern open boundary was specified using an offshore WAVEWATCH III regional dataset (eastern sea, Figure 3a). The use of globally validated WAVEWATCH III wave parameters allowed realistic characterization of offshore wave conditions propagating towards the model domain. A one-dimensional hydrodynamic model was applied to the Han River estuary subdomain, using water levels from a previously calibrated regional model. This model is based on simulations from the "Planning for Fishing Ports and Anchorage Areas for 2021–2030 with a Vision to 2050" project by the Ministry of Agriculture and Rural Development.

#### 3.3.3. Initial Conditions

The model initialization employed a zero-condition baseline for all wave and flow parameters. A 10-day spin-up period was implemented to achieve model equilibrium. TSS background values, derived from averaged measurements at various coastal and project area shore locations, were used to represent initial conditions in the sand transport model. This approach focuses on simulating TSS dispersion primarily from project activities rather than ambient environmental conditions. The MIKE 21MT model's applicability to this site is assumed based on existing literature, compensating for the limitations in site-specific validation data.

#### 3.3.4. Scenario Development for Simulation and Evaluation

The channel maintenance for Tho Quang Port is scheduled for 75 days, beginning with 12 days allocated for equipment transport and setup, followed by 45 days of dredging and disposal of



the dredged material at the authorized location, and concluding with 18 days for inspection and corrections. The project is planned to take place from October 2022 to January 2023, though unforeseen delays such as extreme weather or equipment failures could extend the maintenance period to May 2023. The total volume of dredged material requiring offshore disposal amounts to 654,510 m<sup>3</sup>, and with a 45-day construction timeline, the model applied a maximum daily disposal rate of 29,604 m<sup>3</sup>/day for all simulations to assess worst-case scenarios.

Analysis of long-term meteorological and oceanographic data identified two distinct monsoonal wind regimes that influence hydrodynamics and sediment transport: the Northeast monsoon (December to February) and the Southwest monsoon (June to August). To evaluate their effects on sediment dispersion and deposition, the study conducted separate simulations for each monsoon season, incorporating representative wind, wave, and tidal conditions. During the Northeast monsoon, prevailing winds originate from the Northeast (30–60°) at speeds ranging from 7.2 to 10.5 m/s, generating significant wave heights of 1.2 to 1.8 m with peak periods of 6 to 8 seconds. The tidal range during this season varies from 1.8 to 2.5 m, following a semi-diurnal pattern. Conversely, in the Southwest monsoon, winds predominantly come from the Southwest (210–240°) at speeds between 5.5 and 8.3 m/s, producing lower wave heights of 0.8 to 1.4 m with peak wave periods of 5 to 7 sec. The tidal range is slightly lower, fluctuating between 1.7 and 2.3 m, but also exhibits a semi-diurnal cycle.

For both monsoon scenarios, the maximum daily disposal rate of 29,604 m<sup>3</sup>/day was applied to simulate high-intensity sediment discharge conditions. This approach allowed for a comprehensive assessment of how seasonal variations influence sediment plume transport, dispersion pathways, and seabed deposition, providing critical insights into potential environmental impacts under contrasting monsoonal conditions.

## 4. Model Calibration and Validation

### 4.1. Performance Assessment of the MIKE Model for Coastal Hydrodynamics

The numerical modeling system underwent calibration and validation to ensure reliable simulations of hydrodynamics and sediment transport processes. The coupled hydrodynamic-sediment transport model was calibrated through iterative adjustment and fine-tuning of parameters to optimize agreement between simulated results and observational data, following established techniques [23, 31]. The Nash-Sutcliffe model efficiency coefficient (NSE), a widely-used metric for assessing hydrologic and sediment model performance [32, 33], was utilized to quantify the skill of model predictions. The calibration results from the TT1 location demonstrate the MIKE model's high accuracy in simulating marine hydrodynamic parameters. Across different water depths, the model achieved consistent NSE values of 0.73–0.75 for current speed and flow direction, and 0.69–0.72 for wave height, direction, and cycle. The simulation results show uniform performance from surface to bottom layers, indicating the model's robust capability to capture complex marine dynamics with minimal vertical variation.

The validation results for current speed, flow direction, and wave cycle at the TT2 location are shown in Figures 5–7. Although slightly lower than the calibration results, the validation results are still positive. Current speed and flow direction were well represented throughout the water column (NSE 0.64–0.68 for current speed and NSE 0.65–0.68 for flow direction), capturing the vertical and horizontal flow structures that modulate sediment mixing. While some underestimation of peak velocities occurred, likely due to limitations in resolving fine-scale dynamics, the overall tidal flow patterns were adequately simulated, as found in similar dredging applications [34]. The close agreement between simulated and measured wave (NSE 0.69) and wave cycle (NSE 0.68) provides confidence in modeling the initial



plume dilution (Figure 6), a critical stage in determining sediment footprints. However, the wave height simulation output is relatively lower, with an NSE of 0.56. These validation results for the MIKE model are comparable to the validation achieved in other modeling efforts [6, 35].

The strong model performance benefited from the unstructured flexible mesh allowing high resolution in areas of interest [36],

incorporation of multiple data streams for robust boundary conditions, and coupling of wave-circulation dynamics known to influence sediment advection [18, 23]. Overall, the validation results demonstrate that the modeling system can effectively hindcast observed hydrodynamic conditions in the region, serving as a useful tool for evaluating sediment transport pathways associated with dredging activities.



Figure 5. Comparison of current speed at TT2 location by the MIKE model (red) and observations (black) for the (a) surface layer, (b) the middle layer and (c) the bottom layer of the ocean.

#### 4.2. Configuration of MIKE Model after Calibration

The MIKE model was constructed incorporating an extensive array of parameters to ensure a precise simulation of the system. Fundamental parameters employed in the model encompassed Wind friction ( $Z_{ch}$ ) set at 0.00255, Eddy viscosity at 0.4, Convergence index (CFL) maintained at 0.8, Breaking wave coefficient ( $\gamma$ )

established at 0.8, Horizontal diffusion coefficient set to 1.0, Angle of internal friction of sediment ( $\phi$ ) specified as 30 degrees, and Roughness height maintained at 0.15. These parameters were the result of a fine-tuning process, ensuring that each parameter contributes optimally to the accuracy and reliability of the model in replicating the dynamics of the system under consideration.

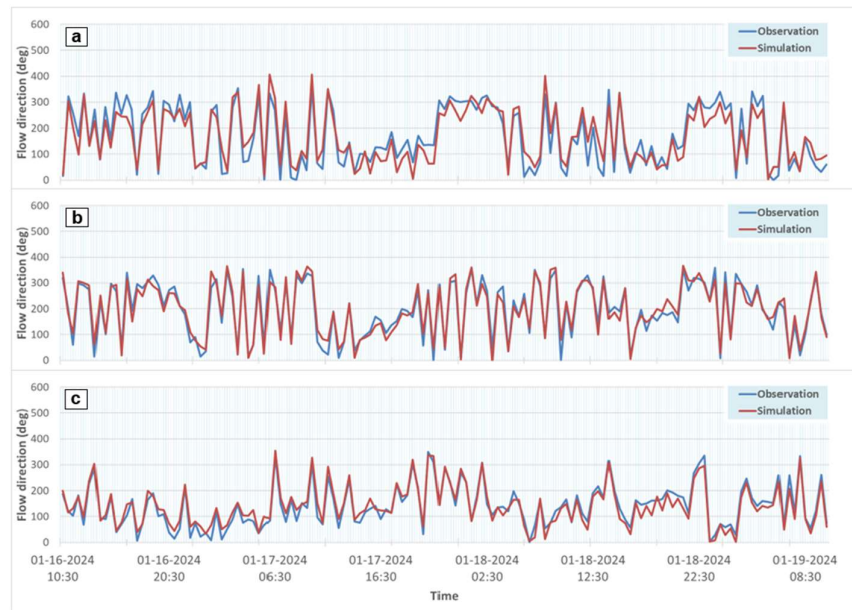


Figure 6. Comparison of water flow direction at TT2 by the MIKE model (red) and observations (blue) for the (a) surface layer, (b) the middle layer and (c) the bottom layer of the ocean.

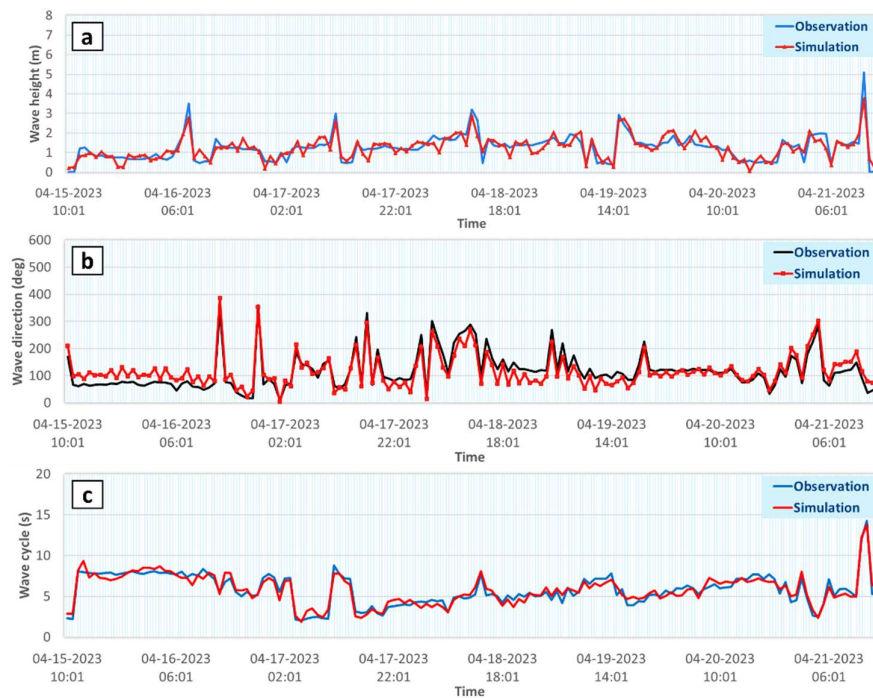


Figure 7. Comparison of (a) wave height, (b) wave direction and (c) wave cycle at TT2 between the MIKE model and observation.

## 5. Result and Discussion

### 5.1. Dispersion of TSS in Sea Water

#### 5.1.1. Hydrodynamic Condition

Hydrodynamics within the dredging area are complex, influenced by river discharge, tides, waves, and embankment structures. In the dry season, tidal currents dominate over low river inflows. High tides instigate flow reversal into

the river, while low tides reinforce outflow. During spring tides, tidal intrusion penetrates far upstream (e.g., Southwest monsoon, Figure 8). In contrast, low tides intensify seaward flow beyond non-tidal conditions. Flow acceleration around the river embankment further complicates hydrodynamics. The embankment splits flow, directing some northward along its length before discharging into the bay, while the remainder flows directly seaward.

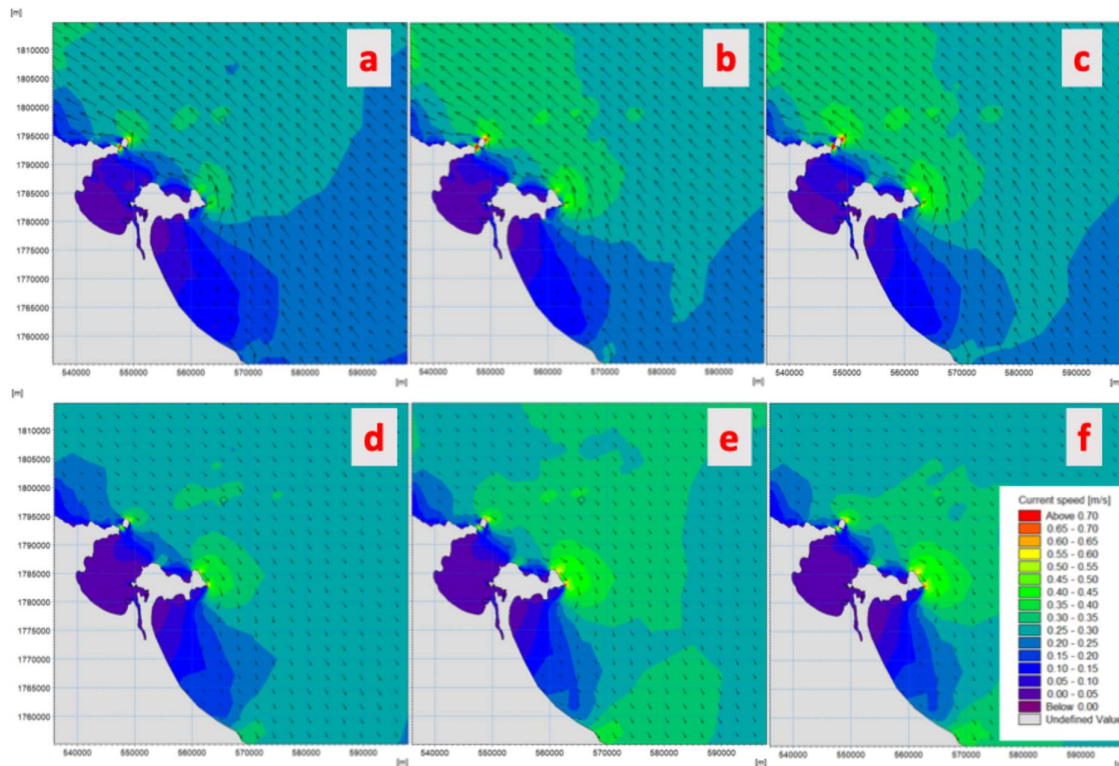


Figure 8. Flow velocity during the Southwest monsoon as simulated by the MIKE model in both the high tide (top images) and low tide (bottom images) phases. The images are organized from left to right, representing the surface, middle, and bottom layers, respectively.

During the Southwest monsoon, heavy river flooding dominates the circulation. Peak river discharge combined with high tides induces temporary upstream surface currents near the river mouth due to the steep water level differences. As the tide retreats, seaward flow becomes more pronounced, though the embankment remains partially submerged due to

prolonged water level differences. This results in complex water flows around the semi-submerged structure. Tide height dynamics reveal an average of 1.4 m far from the coast, with substantially lower heights (typically less than 0.4 m) during coastal high and ebb tide conditions (Figure 9).



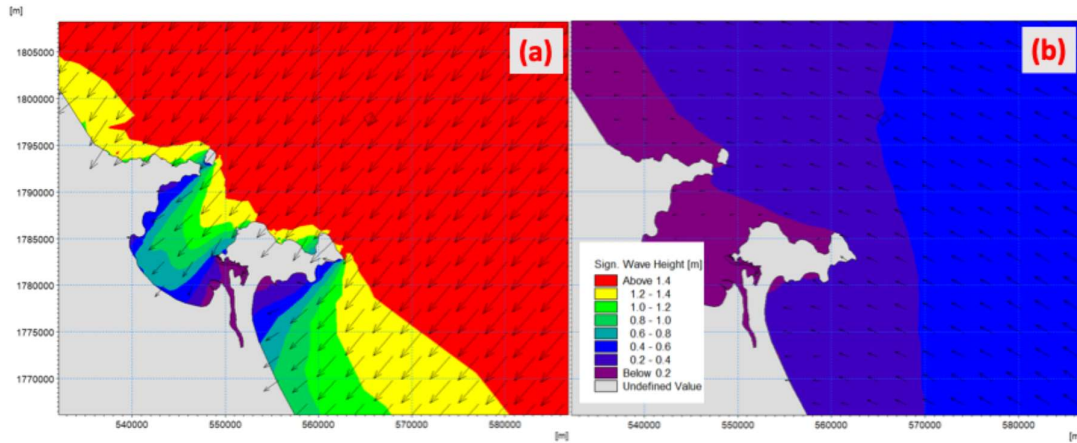


Figure 9. Wave height during the Southwest monsoon as simulated by the MIKE model in both the (a) high tide and (b) low tide phases.

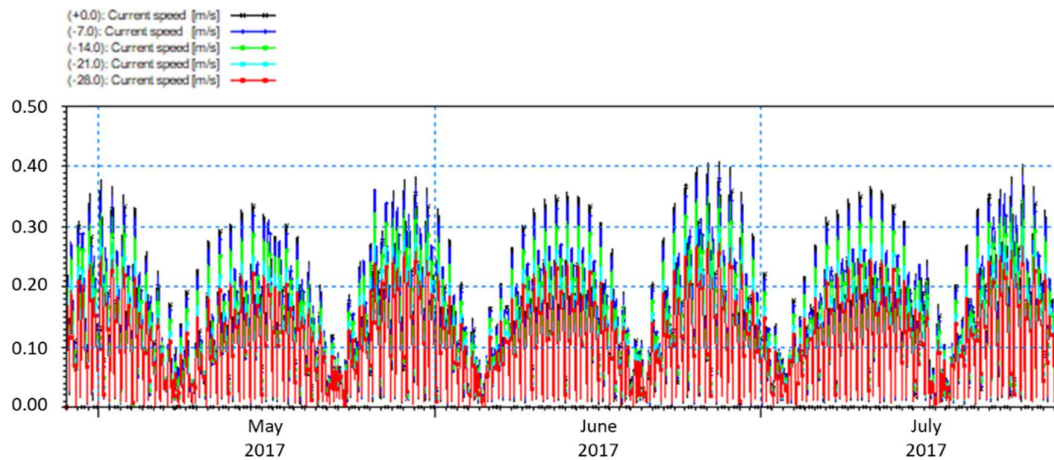


Figure 10. Variation in flow velocity in the submerged area at different verticle layers.

In the offshore disposal site, velocities were extracted at five depths spanning the 0–29 m water column. Similarly, four elevations were sampled within the 6 m dredging area. Analysis showed vertical velocity profiles followed expected physical patterns, with decreasing speed from surface to seabed (Figure 10). This stratification was enhanced during peak flows. Maximum velocities reached approximately 0.42 m/s offshore and 0.28 m/s nearshore. Quantifying velocities in detail provides essential inputs for the model, enabling accurate

simulation of the dispersion and deposition of the disposed dredged material.

#### 5.1.2. Dispersion of TSS in the Submerged Area

The extent and magnitude of suspended sediment plumes generated by the dredged material disposal operations were quantified by simulating TSS transport under contrasting Southwest and Northeast monsoon conditions. Historical wind data from 2022 were used to drive the coupled hydrodynamic-sediment transport models. Model results showed minimal

differences in TSS dispersal patterns between monsoon seasons (Figure 11). In both cases, the primary observed pathway was along the northwest-southeast axis, aligned with prevailing wind and current directions. Dispersion in other directions was limited. Vertically, more extensive TSS dispersal

occurred near the seabed. At the bottom layer, concentrations of  $0.015\text{--}0.02\text{ kg/m}^3$  reached up to 17–18 km northwest and southeast of the disposal site. Areas potentially impacted by higher TSS levels ( $>0.05\text{ kg/m}^3$ ) extended over 12 km. In surface layers, the  $0.015\text{--}0.02\text{ kg/m}^3$  contour propagated less than 13 km.

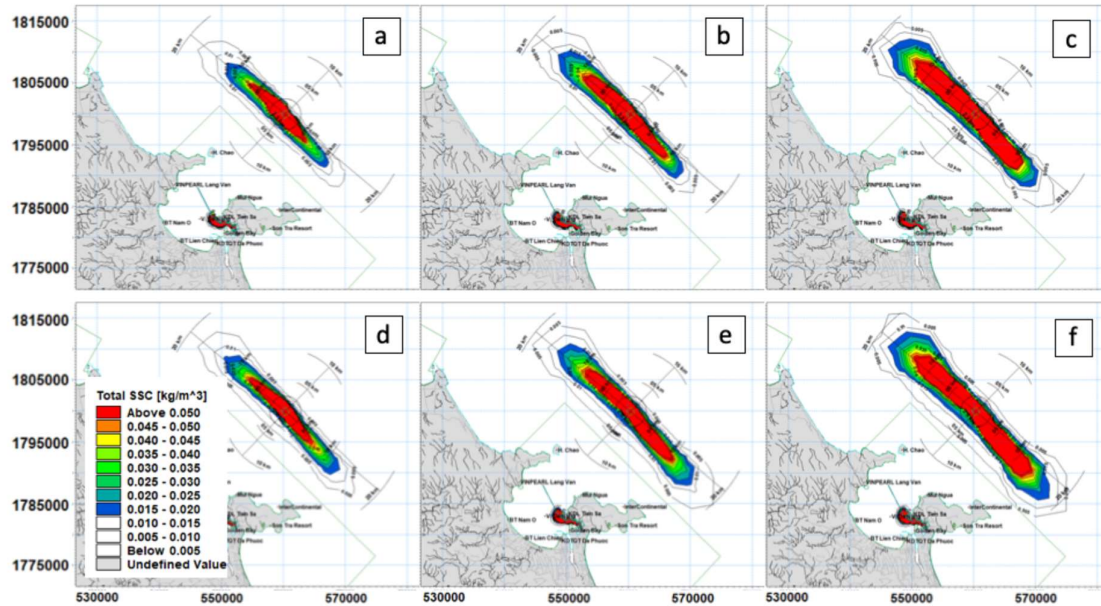


Figure 11. Spatial distribution of peak TSS concentration during the submersion period in the Southwest monsoon (top images) and Northeast monsoon (bottom images). The arrangement of images progresses from left to right, representing the surface, middle, and bottom layers, respectively.

The vertical distribution of suspended solids was further examined by analyzing TSS concentrations along the predominant northwest-southeast dispersion axis, marked by cross-section A-B (Figure 12a). To prevent the dredged material from accumulating in the center of the area, the submersion zone was divided into four equal quadrants (Squares 1–4) as shown in the plan view (Figure 12b). The dredged material was distributed evenly amongst these squares to support consistent construction activities and dispersion modeling. The vertical profile of TSS concentrations over time revealed distinct trends during the disposal operations (Figure 11). TSS levels progressively increased

through the six-week simulation, reaching peak values in week 6 before rapidly declining post-disposal in week 7 (data not shown). Elevated TSS ( $>0.01\text{ kg/m}^3$ ) extended less than 5 km from the source across all weeks, with the highest concentrations ( $>0.05\text{ kg/m}^3$ ) limited to a 2.5–3 km range surrounding the disposal site. This indicates minimal vertical or horizontal dispersion, with dredged sediments depositing rapidly near their release location. The confined suspended sediment plume suggests disposal activities should have a localized influence on water quality and minimal far-field or benthic ecosystem impacts.

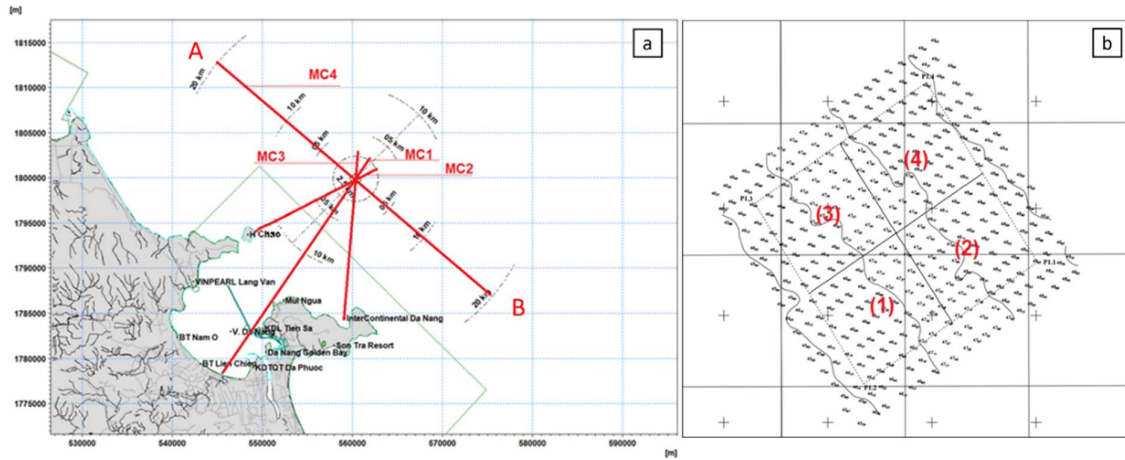


Figure 12. (a) Cross section A-B and (b) the diagram delineating the grid cells in the submerged area.

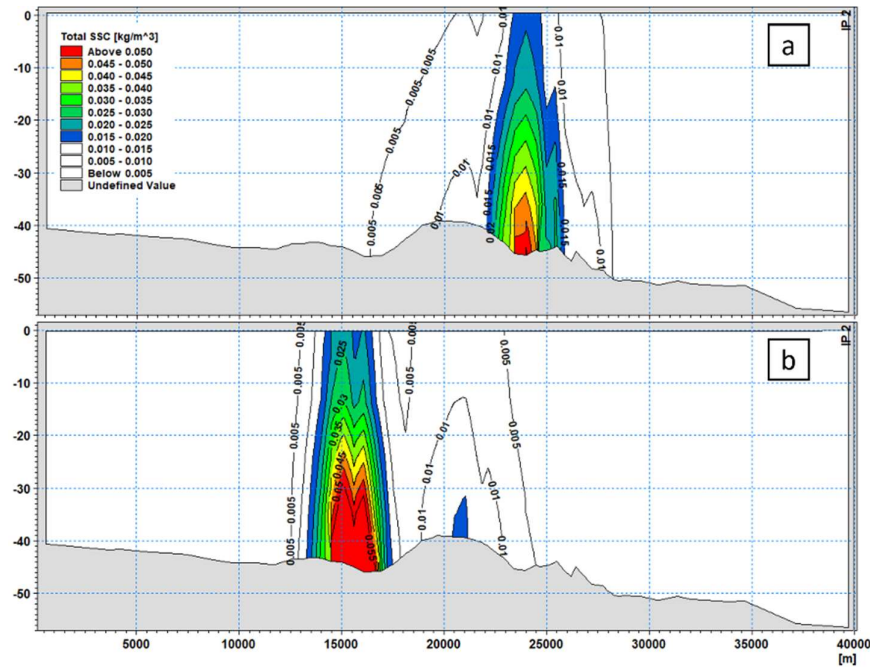


Figure 13. Vertical distribution of TSS along cross-section A-B after (a) one week and (b) six weeks following submersion.

### 5.2. Sedimentation of Dredged Material on Seabed

The division of the disposal area into four equal sections ensures a more uniform sediment deposition, preventing the formation of

excessive seabed elevations that could disrupt the marine environment. Model results revealed similar patterns of seabed morphology following disposal under both monsoon conditions (Figure 12). However, the wind regime noticeably influenced directionality; the Northeast

monsoon instigated a southwesterly shift, while the Southwest monsoon prompted northeast transport. This demonstrates the role of prevailing winds influence the uneven spread of disposed sediment. Only the sand component of the dredged material settled and formed sand dunes on the seabed, while finer components like silt and fine sand dissolved into the seawater and were transported further until diluted in the

marine environment. Visualizations and quantitative data show a cone-shaped depositional profile (data not shown), with maximum elevation approaching 0.4 m per grid cell proximal to the release site. For a 0.1 m contour, the estimated footprint was 102.24 ha during the Southwest monsoon and 121.64 ha in the Northeast monsoon.

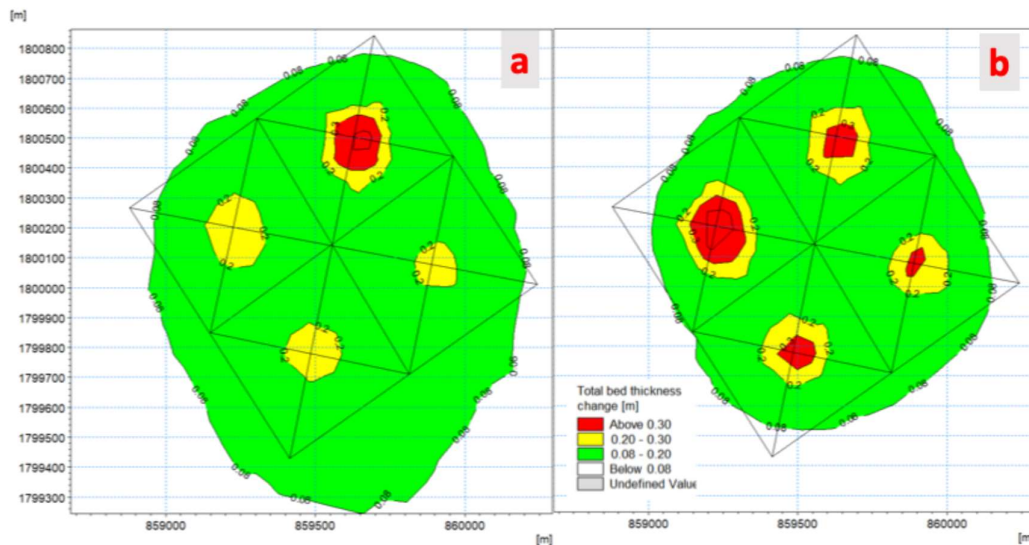


Figure 14. Seabed occupation distribution following the dumping process during the (a) Northeast monsoon and (b) Southwest monsoon seasons.

## 6. Conclusions

This study employed the state-of-the-art MIKE modeling system to comprehensively evaluate the dispersion and sedimentation dynamics associated with the offshore disposal of dredged material from Tho Quang Port. The coupled hydrodynamic-sediment transport simulations provided critical insights into the likely environmental impacts under contrasting monsoon conditions.

The model results showed that TSS dispersal patterns were influenced by monsoonal variations. During the Northeast monsoon, suspended sediments were predominantly transported southwestward, whereas in the Southwest monsoon, the transport shifted

northeastward following the prevailing wind and current directions. Despite these directional differences, the overall extent of elevated TSS concentrations exceeding  $0.05 \text{ kg/m}^3$  remained within a 12 km radius of the disposal site, while lower concentrations ( $0.015\text{--}0.02 \text{ kg/m}^3$ ) extended up to 17–18 km. Importantly, vertical transport of suspended solids was limited to within 5 km of the release location.

Analysis of seabed morphology changes showed a cone-shaped deposition profile reaching a maximum thickness of 0.4 m near the disposal area. The footprint of the 0.1 m accumulation contour varied from 102.24 ha (Southwest monsoon) to 121.64 ha (Northeast monsoon), reflecting the influence of monsoonal currents on sediment deposition. The directional



shift in deposition patterns indicates that while sand particles settled in a localized region, silt and finer sediments were transported further, dispersing more broadly in the marine environment.

These findings highlight the significant role of seasonal wind patterns in shaping the transport and deposition of dredged material. Understanding these influences can help port authorities optimize disposal site selection and environmental monitoring efforts. To further refine the model predictions, future studies should integrate higher-resolution hydrodynamic and sediment transport data, along with ecological impact assessments. By balancing port infrastructure needs with marine conservation, this study demonstrates the utility of advanced numerical modeling to support sustainable dredging practices. The findings provide valuable insights to guide environmental monitoring, impact assessment, and the development of effective management strategies for the disposal of dredged materials.

### Acknowledgments

This study was funded by the research project No. T25-35 of Hanoi University of Mining and Geology.

### Author Contributions

T. A. Q conceptualized the research, developed the literature search protocols, and wrote the manuscript; N. D. T helped conceptualize the paper, conducted data analysis, and assisted with writing; T. T. T and L. D. N performed the literature search and data analysis. All authors discussed the results and contributed to the manuscript's writing.

### References

- [1] H. Tanaka, V. C. Hoang, V. T. Nguyen, Investigation of Morphological Change at the Cua Dai River Mouth Through Satellite Image Analysis, Coastal Engineering Proceedings, Vol. 35, 2017, <https://doi.org/10.9753/icce.v35.sediment.9>.
- [2] D. V. Vu, D. L. Tran, Impact of Wave Conditions on Sediment Transport Characteristics and Seabed Morphology Changes in the Coastal Estuary of Hai Phong. Journal of Marine Science and Technology, Vol. 18, No. 1, 2018, <https://doi.org/10.15625/1859-3097/18/1/9045>.
- [3] D. N. Quang, N. Q. D. Anh, H. S. Tam, N. X. Tinh, H. Tanaka, N. T. Viet, Evaluation of Cua Lo Estuary's Morpho-Dynamic Evolution and Its Impact on Port Planning, Journal of Marine Science and Engineering, Vol. 11, No. 3, 2023, <https://doi.org/10.3390/jmse11030611>.
- [4] T. D. Lan, V. D. Vinh, D. T. T. Huong, D. G. Khanh, Assessment of the Ability to Select the Position for Dredging Material and Navigating Maritime Traffic in the Sea Area of Hai Phong Port, Journal of Marine Science and Technology, Vol. 19, No. 4, 2020, <https://doi.org/10.15625/1859-3097/19/4/12713>.
- [5] F. Samsami, S. A. Haghshenas, M. Soltanpour, Physical and Rheological Characteristics of Sediment for Nautical Depth Assessment in Bushehr Port and Its Access Channel, Water, Vol. 14, No. 24, 2022, <https://doi.org/10.3390/w14244116>.
- [6] N. T. H. Ngoc, T. A. Quan, The Dispersion of Total Suspended Solids in Seawater Following Submersion of Dredged Material in the Vung Ang Port, Vietnam Journal of Agricultural Sciences, Vol. 6, No. 4, 2023, <https://doi.org/10.31817/vjas.2023.6.4.04>.
- [7] J. A. Zyserman, J. Fredsøe, Data Analysis of Bed Concentration of Suspended Sediment, Journal of Hydraulic Engineering, Vol. 120, No. 9, 1994, [https://doi.org/10.1061/\(ASCE\)0733-9429\(1994\)120:9\(1021\)](https://doi.org/10.1061/(ASCE)0733-9429(1994)120:9(1021)).
- [8] J. P. M. Syvitski, Y. Saito, Morphodynamics of Deltas Under the Influence of Humans, Global and Planetary Change, Vol. 57, No. 3, 2007, <https://doi.org/10.1016/j.gloplacha.2006.12.001>.
- [9] M. Prumm, I. Gregorio, Impacts of Port Development on Estuarine Morphodynamics: Ribadeo (Spain), Ocean & Coastal Management, Vol. 130, 2016, <https://doi.org/10.1016/j.ocecoaman.2016.05.003>.
- [10] N. Kamal, S. Nahla, Evaluating and Analyzing Navigation Efficiency for the River Nile (Case Study: Ensa-Naga Hamady Reach), Ain Shams Engineering Journal, Vol. 9, No. 4, 2018, <https://doi.org/10.1016/j.asej.2017.08.006>.

- [11] E. L. Jackson, B. English, A. D. Irving, A. M. Symonds, G. Dwane, O. T. Nevin, D. T. Maher, A Multifaceted Approach for Determining Sediment Provenance to Coastal Shipping Channels, *Journal of Marine Science and Engineering*, Vol. 7, No. 12, 2019, <https://doi.org/10.3390/jmse7120434>,
- [12] R. Firmansyah, M. Z. Jauzi, D. C. Istiyanto, A. Subarkah, S. U. Sujoko, M. Wibowo, R. C. Yuniardi. Study on the Design and Implementation of BPPT-Lock Armored Groin for Sediment Control Structure in Front of Sea Water Intake, *Zona Laut Jurnal Inovasi Sains Dan Teknologi Kelautan*, Vol. 4, No. 3, 2023, <https://doi.org/10.62012/zt.v4i3.28244>.
- [13] E. Espagne, T. N. Duc, M. H. Nguyen, E. Pannier, M. N. Woillez, A. Drogoul, T. P. L. Huynh, T. T. Le, T. T. H. Nguyen et al., Climate Change in Vietnam, Impacts and Adaptation: A COP26 Assessment Report of the GEMMES Vietnam Project, Agence Française de Développement, 2021.
- [14] Q. T. Anh, T. N. Duc, E. Espagne, L. T. Tuan, A High-Resolution Projected Climate Dataset for Vietnam: Construction and Preliminary Application in Assessing Future Change, *Journal of Water and Climate Change*, Vol. 13, No. 9, 2022, <https://doi.org/10.2166/wcc.2022.144>.
- [15] Q. T. Anh, T. N. Duc, E. Espagne, L. T. Tuan, A 10-km CMIP6 Downscaled Dataset of Temperature and Precipitation for Historical and Future Vietnam Climate, *Scientific Data*, Vol. 10, No. 1, 2023, <https://doi.org/10.1038/s41597-023-02159-2>.
- [16] T. C. Vu, V. T. Mai, B. N. Nguyen, V. D. Nguyen, T. Hoang, The Interaction of Tide and River Flow on Water Quality in Hai Phong Coastal Waters (Lach Huyen-Do Son) Drawn from Field Observation, *Vietnam Journal of Marine Science and Technology*, Vol. 23, No. 2, 2023, <https://doi.org/10.15625/1859-3097/17997>.
- [17] N. Q. D. Anh, D. C. Dien, H. S. Tam, N. T. Viet, H. Tanaka, Numerical Simulation of Hydrodynamic and Sediment Transport at Cua Lo Inlet, Quang Nam Province, Vietnam, In *Proceedings of the 8<sup>th</sup> International Conference on the Application of Physical Modelling in Coastal and Port Engineering and Science*, 2020, pp. 51-60, 2020.
- [18] J. R. Cox, J. Lingbeek, S. A. H. Weisscher, M. G. Kleinhan, Effects of Sea-Level Rise on Dredging and Dredged Estuary Morphology, *Journal of Geophysical Research: Earth Surface*, Vol. 127, No. 10, 2022, <https://doi.org/10.1029/2022JF006790>.
- [19] D. H. Wilber, D. G. Clarke, Biological Effects of Suspended Sediments: A Review of Suspended Sediment Impacts on Fish and Shellfish with Relation to Dredging Activities in Estuaries. *North American Journal of Fisheries Management*, Vol. 21, No. 4, 2001, [https://doi.org/10.1577/1548-8675\(2001\)021<0855:BEOSSA>2.0.CO;2](https://doi.org/10.1577/1548-8675(2001)021<0855:BEOSSA>2.0.CO;2).
- [20] V. L. G. Todd, I. B. Todd, J. C. Gardiner, E. C. N. Morrin, N. A. MacPherson, N. A. DiMarzio, F. Thomsen, A Review of Impacts of Marine Dredging Activities on Marine Mammals. *ICES Journal of Marine Science*, Vol. 72, No. 2, 2015, <https://doi.org/10.1093/icesjms/fsu187>.
- [21] S. G. Bolam, H. L. Rees, P. Somerfield, R. Smith, K. R. Clarke, R. Atkins, E. G. M. Warwick, M. Arnacho, Ecological Consequences of Dredged Material Disposal in the Marine Environment: A Holistic Assessment of Activities Around the England and Wales Coastline. *Marine Pollution Bulletin*, Vol. 52, No. 4, 2006, <https://doi.org/10.1016/j.marpolbul.2005.09.028>.
- [22] P. L. A. Erftemeijer, R. R. R. Lewis, Environmental Impacts of Dredging on Seagrasses: A Review. *Marine Pollution Bulletin*, Vol. 52, No. 12, 2006, <https://doi.org/10.1016/j.marpolbul.2006.09.006>.
- [23] T. A. Quan, D. T. Hai, N. T. H. Ngoc, The Dispersion of Suspended Matter in Seawater Caused by Dredging and Disposal of Dredged Materials at Nghi Son Port, Thanh Hoa, *Journal of Environment*, Vol. II, 2021.
- [24] D. V. Duy, H. Tanaka, Y. Mitobe, N. Q. D. Anh, N. T. Viet, Sand Spit Elongation and Sediment Balance at Cua Lo Inlet in Central Vietnam, *Journal of Coastal Research*, Vol. 81, No. sp1, 2018, <https://doi.org/10.2112/SI81-005.1>.
- [25] J. Lin, X. M. Xu, Y. Chen, Q. Z. Zhou, L. R. Yuan, Q. Zhu, J. H. Wang, Distribution and Composition of Suspended Matters in the Wintertime in the East China Sea, *Science of the Total Environment*, Vol. 664, 2019, <https://doi.org/10.1016/j.scitotenv.2019.02.021>.
- [26] T. Nagasawa, M. T. T. Thuy, N. T. Viet, H. Tanaka, Analysis of Shoreline Change in Cua Dai Beach by Using Empirical Orthogonal Function, *Coastal Engineering Journal*, Vol. 60, No. 4, 2018, <https://doi.org/10.1080/21664250.2018.1554202>.
- [27] M. Bortali, M. Rabouli, M. Yessari, A. Hajjaji, Characterizing Harbor Dredged Sediment for Sustainable Reuse as Construction Material, *Sustainability*, Vol. 15, No. 3, 2023, <https://doi.org/10.3390/su15031834>.

- [28] P. Ren, B. D. Bornhold, D. B. Prior, Seafloor Morphology and Sedimentary Processes, Knight Inlet, British Columbia, Sedimentary Geology, Vol. 103, No. 3-4, 1996, [https://doi.org/10.1016/0037-0738\(95\)00090-9](https://doi.org/10.1016/0037-0738(95)00090-9).
- [29] T. A. Rydningen, J. S. Laberg, V. Kolstad, Seabed Morphology and Sedimentary Processes on High-Gradient Trough Mouth Fans Offshore Troms, Northern Norway, Geomorphology, Vol. 246, 2015, <https://doi.org/10.1016/j.geomorph.2015.06.007>.
- [30] DHI, MIKE Power by DHI, 2017, <https://www.mikepoweredbydhi.com/products/mike-3-wave-fm> (accessed on: September 1<sup>st</sup>, 2024).
- [31] K. Purkiani, B. Gillard, A. Paul, M. Haeckel, S. Haalboom, J. Greinert, H. D. Stigter, M. Hollstein, M. Baeye, A. Vink, L. Thomsen, M. Schulz, Numerical Simulation of Deep-Sea Sediment Transport Induced by a Dredge Experiment in the Northeastern Pacific Ocean, Frontiers in Marine Science, Vol. 8, 2021, <https://doi.org/10.3389/fmars.2021.719463>.
- [32] J. E. Nash, J. V. Sutcliffe, River Flow Forecasting Through Conceptual Models Part I — A Discussion of Principles. Journal of Hydrology, Vol. 10, No. 3, 1970, [https://doi.org/10.1016/0022-1694\(70\)90255-6](https://doi.org/10.1016/0022-1694(70)90255-6).
- [33] C. J. Willmott, S. M. Robeson, K. Matsuura, A Refined Index of Model Performance. International Journal of Climatology, Vol. 32, No. 13, 2012, <https://doi.org/10.1002/joc.2419>.
- [34] R. L. Mille, Modeling Response of Water Temperature to Channelization in a Coastal River Network, River Research and Applications, Vol. 37, No. 3, 2021, <https://doi.org/10.1002/rra.3756>.
- [35] J. M. Preston, D. R. Parrott, W. T. Collins, Sediment Classification Based on Repetitive Multibeam Bathymetry Surveys of an Offshore Disposal Site, Oceans 2003. Celebrating the Past, Teaming Toward the Future, Vol. 1, pp. 69-75, 2003, <https://doi.org/10.1109/OCEANS.2003.178523>.
- [36] W. Yuwei, Z. Hui, H. Jun, R. Xingyue, X. Xiang, Finite Element Study on Temperature Field of Underwater Dredging Devices via the Artificial Ground Freezing Method, Geofluids, Vol. 2022, Article ID 7502693, 2022, <https://doi.org/10.1155/2022/7502693>.